

Resonant three-level saturation spectroscopy in a fast, accelerated atom beam

O. Poulsen, P. Nielsen, U. Nielsen, and P. S. Ramanujam*
Institute of Physics, University of Aarhus, DK-8000 Aarhus C, Denmark

N. I. Winstrup
Project Group of Physics, Aalborg University Center, DK-9000 Aalborg, Denmark
 (Received 16 June 1982)

Resonant-saturation spectroscopy has been carried out in both the V configuration and the inverted- V configuration in fast, accelerated atom beams of Ne I^* and Ca I^* . Hole (peak) creation in the velocity distributions are shown to yield resonances Doppler free to first order in a collinear geometry, which allows high spectral stability and resolution. Wave numbers for three optical transitions in ^{20}Ne are reported.

I. INTRODUCTION

During the last ten years, fast-beam—laser spectroscopy has experienced a rapid development. Since the first demonstration of laser-induced fluorescence by means of Doppler tuning,¹ many refined techniques have been introduced, all concerned with the unique possibilities offered by the fast-moving absorbers. The most important feature is related to longitudinal cooling² exploited in collinear fast-beam—laser interactions.^{3,4} Linewidths approaching the natural widths are obtained, mainly limited by the velocity spread of the ions or atoms due to high-voltage fluctuations. This method has been used to study nuclear properties⁵ as well as Lamb shifts in high- Z , one- and two-electron atoms,⁶ representing two extreme applications of this technique. By using a modulated-laser field lifetimes can be obtained⁷ together with g_J values⁸ in a time-differential level-crossing scheme. The ultimate in using the time resolution offered by the fast-moving absorbers is the optical Ramsey fringes recently observed,⁹ giving promise of very high, sub-natural resolution.

However, despite the high inherent resolution due to the velocity compression, these methods are still not Doppler free. The first experiment, which demonstrated a Doppler-free, saturated absorption using a perpendicular fast-beam laser interaction,¹⁰ was soon followed by “in-flight” saturated absorption using Doppler labeling¹¹ and thus taking full advantage of the near-“monovelocity” Doppler-tuning capability in the fast ionic beam and with the hole burning depending on a convolution of the natural or power-broadened linewidth with the velocity distribution.¹² In the limit of very broad velocity distributions, the burned holes will be limited only by the natural decay width and with an absolute po-

sition shifted by the total Doppler effect.

From a spectroscopy point of view, a more desirable situation is the complete elimination of the first-order Doppler shift. Resonant two-photon absorption¹³ in a fast, accelerated atom beam offers this possibility, yielding a two-photon resonance broadened only by the second-order Doppler effect. The frequency stability of this resonance is very high for suitable Rabi frequencies and with only modest laser-power broadenings. In the $3s[\frac{3}{2}]_2-4d'[\frac{5}{2}]_3$ two-photon absorption in a 119-kV Ne I^* atom beam, a linewidth of 2.3 MHz was obtained, limited only by the natural width of the $4d'$ level representing the highest optical resolution obtained in fast-beam laser spectroscopy so far.

The same attractive features can be obtained in a saturated-absorption experiment on fast, accelerated atoms. In a classical-saturation experiment, the atoms with zero longitudinal velocity components are selected, thus eliminating the first-order Doppler effect.

In a fast, accelerated atom beam with a high average velocity and a low longitudinal velocity spread, it is not possible with a single laser to saturate and probe on the same transition in a collinear geometry due to the large Doppler shifts. However, a V configuration can be realized, using *one* laser retroreflected along the fast atom beam, with the excited velocity classes $\beta_a=(v_a/c)$ determined by

$$\begin{aligned}\sigma_1 &= \sigma_L \gamma(\beta_a)(1-\beta_a), \\ \sigma_2 &= \sigma_L \gamma(\beta_b)(1+\beta_b),\end{aligned}\tag{1}$$

where σ_L is the laser wave number, σ_i is the atomic-transition energies, and $\gamma(\beta)=(1-\beta^2)^{-1/2}$. The situation is shown in Fig. 1(a). For a particular particle velocity $\beta_a=\beta_b=\beta$, given by

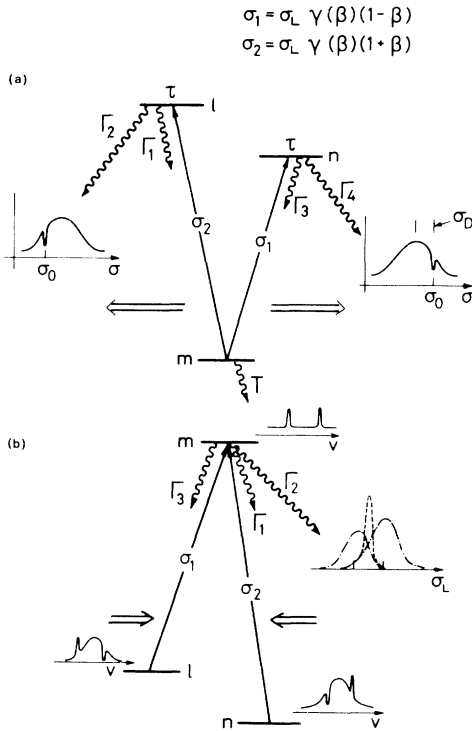


FIG. 1. Simplified energy-level diagrams of the two configurations studied. (a) The V configuration and (b) the inverted- V configuration. Simultaneous excitation on the two transitions are obtained using a laser wave number σ_L and a velocity $\beta = v/c$ of the fast-moving absorbers, satisfying the relations $\sigma_1 = \sigma_L \gamma(\beta)(1 - \beta)$ and $\sigma_2 = \sigma_L \gamma(\beta)(1 + \beta)$.

$$\beta = \frac{\sigma_2 - \sigma_1}{\sigma_2 + \sigma_1}, \quad (2)$$

the laser field (with wave number σ_L) is resonant on both transitions and interacts with the same velocity class in the initial level. This hole burning, which is Doppler free to first order and limited only by the homogeneous linewidth, manifests itself through a reduction in population of both the excited levels.

The situation with the resonant inverted- V configuration is similar, with the basic energy-level scheme shown in Fig. 1(b). The laser field burns holes in the velocity distribution of the two metastable levels at velocities β_a and β_b given by Eq. (1), and, neglecting recoil, corresponding peaks are created in the velocity distribution of the excited level. Due to a strong spontaneous coupling between the excited and metastable levels, the peaks in the velocity distribution of the excited level will manifest themselves as additional peaks in the velocity distributions of the two lower metastable levels. At resonance, given by Eq. (2), the holes and peaks collapse and give rise to an increased emission, Doppler free to first order and

with a linewidth limited only by the homogeneous width, which is given by $1/\tau + 2/T$, where T is the transit time and τ the excited-level lifetime. A resonant stimulated Raman scattering will also take place at sufficiently high Rabi frequencies.

II. APPARATUS

The experimental apparatus used to observe these saturated-absorption profiles has been described previously.¹³ A 300-kV isotope separator produces pure ionic beams, which can be postaccelerated and neutralized in a sodium metal vapor cell. A laser field from a stabilized cw-dye ring laser is superimposed with the fast atom beam in a collinear geometry and reflected back onto itself by a curved mirror. This return field is chopped, and the two spectra, with both fields, respectively, only the forward field, driving the σ_1 transition present, are recorded with the use of a computer-controlled digital lock-in multiscaling data-acquisition system, which also sweeps the laser frequency.

III. EXPERIMENTAL

The three main features of the experiment are effective hole burning, natural width of the resonances, and elimination of the first-order Doppler shift. In Fig. 2 is shown a typical resonance obtained in NeI at 263.715 kV. In curve b is shown the resonance with only *one* laser field, and in curve a is seen the same profile, but now the laser field is retroreflected onto itself, probing the hole in the Doppler velocity profile. This hole is so deep that all atoms with velocity β , given by Eq. (2), are pumped out from the initial level. Also, the width of the hole is substantially smaller than the residual Doppler width of the atoms, allowing a resolution limited only by the natural-decay width. By changing the velocity, it is easily demonstrated that the observed holes are Doppler free to first order. In Fig. 3 are shown three resonances, once again obtained in a V configuration in NeI* at a beam energy around 61.763 kV. It is seen that the broad Doppler profile is shifted due to the total Doppler effect, whereas the burnt hole is dependent only on the second-order Doppler shift. This fact is further substantiated in Fig. 4, where the solid curve represents the total Doppler shift, which solely accounts for the energy detuning between the hole and the Doppler profile. That no ac Stark shifts are observed is consistent with our experimental parameters: small symmetric laser detunings and equal Rabi frequencies on the two transitions.

For the inverted- V configuration [Fig. 1(b)], the same features are observed. Instead of a hole, an increased emission is observed when the two velocity

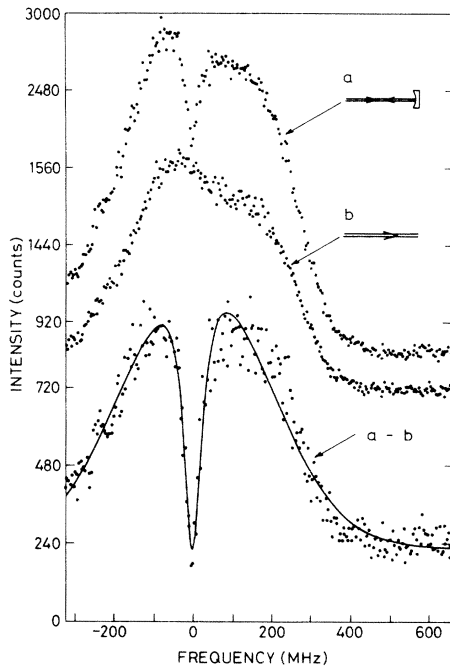


FIG. 2. The $3s[\frac{3}{2}]_2-(3p'[\frac{3}{2}]_2, 3p'[\frac{1}{2}]_1)$ resonance found at $\sigma_L = 16\,906.401(2) \text{ cm}^{-1}$ and a particle energy of $E = 263.715 \text{ kV}$. Curve b shows the resonance obtained for the resonance with only *one* active laser field, whereas the laser beam is retroreflected in curve a. The difference is shown in curve a-b. Width of the saturated dip, Doppler free to first order, is 36 MHz with a natural width of $\simeq 11 \text{ MHz}$.

classes representing the hole and the peak coincide. This is demonstrated in Fig. 5 by means of the $(4s4p^3P_2, 4s4p^3P_1)-4s5s^3S_1$ transitions in Ca I. The increase in emission is also here Doppler free to first order and limited only by the natural linewidth of the upper level.

IV. DISCUSSION

These phenomena are well known from studies on thermal absorbers, either by probing or pumping on the same transition with the same laser, or by using two laser fields on two separate transitions.^{14,15}

In the presence of optical pumping, these phenomena are strongly modified,¹⁶ depending on the polarization of the laser fields and the branching ratios of the upper excited levels. In the present work, linearly polarized light has been used to avoid a redistribution of the population among the M -quantum states of the initial levels, whereas the branching ratios for decays from the upper levels (Fig. 1) favor transitions out. Thus the saturation parameter is reduced considerably.¹⁶ To study the hole burning in more detail, the density matrix for

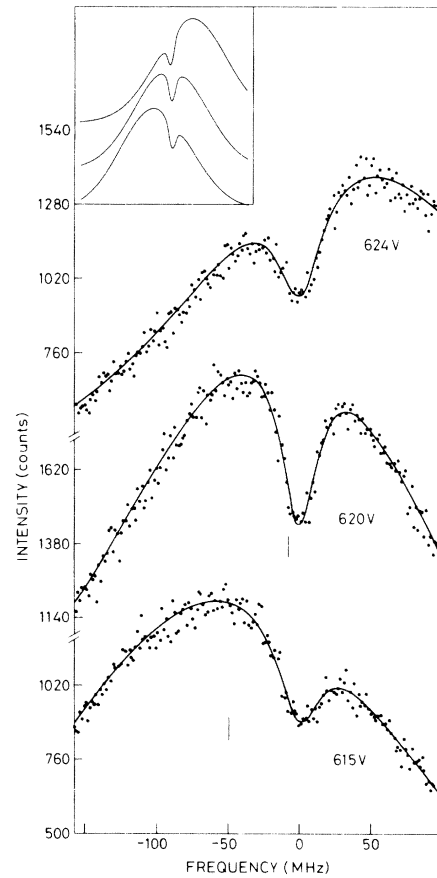


FIG. 3. The $3s[\frac{3}{2}]_2-(3p'[\frac{3}{2}]_2, 3p'[\frac{3}{2}]_1)$ resonance found at $\sigma_L = 16\,773.413(2) \text{ cm}^{-1}$. Three resonances are obtained for different energies (velocity) of the atom beam, showing that the hole burning is Doppler free to first order. Actual energies are given $(61\,142 + \delta V)V$, where δV is the postacceleration, also given in the figure. In the inset is shown spectra which are calculated, using Eq. (3) with Rabi frequencies $\Omega_1 = 12 \text{ MHz}$, $\Omega_2 = 25 \text{ MHz}$, and $T = 500 \text{ ns}$, representing the experimental conditions.

these three-level systems has been solved numerically with the proper branching ratios and decay constants being allowed for, as well as taking into account the fast-beam kinetics, as given in Eq. (1), and finally integrated over the velocity distribution of the fast, accelerated atoms.

The density-matrix elements are given by

$$\frac{d}{dt}\hat{\rho} = -i/\hbar[\kappa_0 - \vec{\mu} \cdot \vec{E}, \hat{\rho}] + R, \quad (3)$$

where κ_0 is the atomic Hamiltonian, $-\vec{\mu} \cdot \vec{E}$ is the interaction term with the field, and R represents incoherent relaxation terms. As an example, using the rotating-wave approximation, the component ρ_{mm} in the V configuration becomes

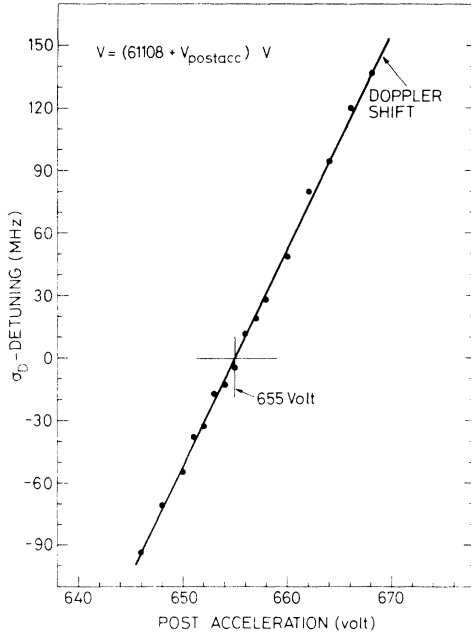


FIG. 4. The energy detuning σ_D , representing the separation between the Doppler-free hole burning and the Doppler-broadened absorption profile, plotted against the beam energy eV. Solid curve represent the total Doppler shift.

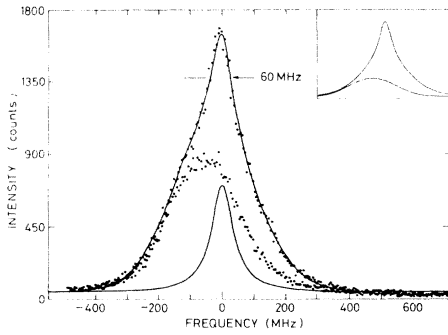


FIG. 5. An enhanced emission, Doppler free to first order, is observed in the inverted- V configuration. Shown is the Doppler-broadened transition obtained with only one laser field active, as well as the total emitted light, with the laser beam retroreflected along the fast atom beam. Solid curve represents a fit with two Gaussian profiles and one Lorentzian profile to take into account the two Doppler-broadened, direct excitations as well as the increased emission, due to the creation of holes and peaks in the velocity distribution of the two initial levels [see Fig. 1(b)]. Lorentzian is separately drawn below, having a width of 60 MHz corresponding to an excited-state lifetime of 15 ns and Rabi frequencies of $\Omega_1=61$ MHz and $\Omega_2=80$ MHz. Prediction of Eq. (3), with the proper velocity integration taken into account, and using these Rabi frequencies and $T=400$ ns as well as the same resonance with $\Omega_2 \equiv 0$, i.e., the retroreflected laser field blocked, is shown in the inset.

$$\begin{aligned} \frac{d}{dt}\rho_{mm} = & 1/T(n_m^{(0)} - \rho_{mm}) + \Gamma_1\rho_{ll} + \Gamma_3\rho_{nn} \\ & + i\Omega_1(\rho_{mn} - \rho_{nm}) + i\Omega_2(\rho_{ml} - \rho_{lm}), \end{aligned} \quad (4)$$

where Γ_1, Γ_3 are the decay rates from level l, n to the metastable level m , and Ω_i is the Rabi frequency given by $\vec{\mu}_i \cdot \vec{E}_i / 2\hbar$, $n_m^{(0)}$ is the initial population in level m . Transit-time effects are included as an effective lifetime of the metastable level as well as an increase of the width of the upper levels n, l given by $1/\tau + 1/T$. The homogeneous linewidth γ is thus given by

$$\gamma = \frac{1}{\tau} + \frac{2}{T}. \quad (5)$$

The transit time T is variable in our experiment, ranging from 300 to 800 ns.

Equation (3) can easily be solved under steady-state conditions, using known transition rates Γ_i (Ref. 17), particle velocity, and dispersion as well as laser intensity. In the inset of Fig. 3 are shown such simulated spectra obtained after velocity integration. Of particular interest are the broadening and shift parameters. Equation (3) predicts, after velocity integration, a homogeneous linewidth of the burnt hole of

$$\gamma_{\text{eff}} = \frac{\gamma_l}{2} \left[1 + \frac{\Omega_2^2}{\Omega_{20}^2} \right]^{1/2} + \frac{\gamma_n}{2} \left[1 + \frac{\Omega_1^2}{\Omega_{10}^2} \right]^{1/2}, \quad (6)$$

where Ω_{i0} are the reduced Rabi saturation parameters¹⁶ given by

$$\begin{aligned} \Omega_{10}^2 &= \frac{\gamma_n(1/\tau + 1/T)}{4(2 + \Gamma_4 T)}, \\ \Omega_{20}^2 &= \frac{\gamma_l(1/\tau + 1/T)}{4(2 + \Gamma_2 T)}. \end{aligned} \quad (7)$$

τ is the lifetime of the upper levels, and Γ_2, Γ_4 are the transition rates out of the V configuration. Equation (7) predicts a sizeable reduction in saturation intensity. This is a valuable feature as it is possible effectively to burn holes with low laser powers and thus make possible a sizable expansion of the laser field to ensure plane wave fronts and long interaction times T .

The second systematic effect to consider is the ac Stark shift. From Eq. (3), one obtains¹⁸ a shift δ of

$$\delta = -\frac{\Delta\Omega_1^2}{\Delta^2 + \gamma^2} - \frac{\Delta'\Omega_2^2}{\Delta'^2 + \gamma^2},$$

where $\Delta = \omega - kv - \omega_{nm}$, and $\Delta' = \omega + kv - \omega_{lm}$ are the laser detunings on the two transitions, and the

TABLE I. Wave numbers in $^{20}\text{Ne I}$.

Transition	σ (cm $^{-1}$)	σ (cm $^{-1}$) (Ref. 19)	σ (cm $^{-1}$) (Ref. 20)	σ (cm $^{-1}$) (Ref. 21)
$3s[\frac{3}{2}]_2-3p'[\frac{3}{2}]_2$	16 816.667(2)	16 816.668	16 816.673(9)	16 816.666 34(2)
$3s[\frac{3}{2}]_2-3p'[\frac{3}{2}]_1$	16 730.269(2)	16 730.272	16 730.275(6)	
$3s[\frac{3}{2}]_2-3p'[\frac{1}{2}]_1$	16 996.613(2)	16 996.612	16 996.616(8)	16 996.611 85(2)

Ω_i are the Rabi frequencies, respectively. Here, γ is again the homogeneous width of the hole burnt. The second-order broadening is neglected.

There are several cases of interest. (a) Symmetric detuning $\Delta = -\Delta'$ yielding

$$\delta = \frac{\Delta(\Omega_1^2 - \Omega_2^2)}{\Delta^2 + \gamma^2} \equiv 0$$

for equal Rabi frequencies. Symmetric detuning is easily accomplished by choosing a particle velocity β given by Eq. (2). (b) $\delta \equiv 0$ for $\Delta\Omega_1^2 \simeq -\Delta'\Omega_2^2$, which can be carried out only for velocities v within the Doppler profile. With an energy spread of $\delta\beta \simeq 10$ V, a difference of $\simeq 10\%$ in Rabi frequencies can be compensated for. The case of symmetric detuning $\Delta + \Delta' = 0$ can easily be accomplished because of our complete velocity control. The ac Stark shift can then be eliminated even with $\Omega_1 \neq \Omega_2$, where only a broadening takes place around $\Delta = -\Delta' = 0$. With our experimental parameters, we find a broadening $\delta_{\max} \approx 2$ MHz, in agreement with Fig. 4, where only the Doppler effect explains the observed detunings.

The inverted- V configuration in Ca I^* can be calculated in a similar manner. The main difference with the Ne I^* cases is the ratio $(\Gamma_1 + \Gamma_3)/\Gamma_2 \simeq 9$, i.e., a much more closed system with a correspondingly smaller reduction in effective saturation parameters. The inset in Fig. 5 shows a calculation of the scattered intensity, proportional to ρ_{mm} , yielding good agreement with experiment.

However, one problem, which is not taken into account in this calculation, needs further attention. Most important is that we never reach steady-state conditions. With the high velocity of the atomic absorbers, our experiment is time differential with optical-pumping processes taking place separated in time from observation of the scattered light further down along the beam. Being a one-dimensional gas with negligible collisional repopulation, this fast beam thus requires a time-dependent solution to the

equations of motion, allowing a description of the time-dependent hole (peak) burning *along* the beam, both by the two laser fields, separately as well as by their combined effect in burning holes Doppler free to first order.

V. RESULTS

By using these Doppler-free methods, precision wave numbers for three transitions in $^{20}\text{Ne I}$ have been obtained. The results have been summarized in Table I together with the classical-spectroscopy results of Kaufman and Edlén¹⁹ and the more recent measurements of Hall and Lee²⁰ and Juncar and Pinar.²¹ Our results demonstrate the possibilities of performing optical measurements, which are limited *only* by the absolute accuracy of our λ meter, but which are *not* dependent on the velocity to first order. The second-order Doppler broadening amounts to $\simeq 1$ MHz, which is negligible compared to the natural-decay widths.

VI. CONCLUSION

To fully appreciate the resolution and possibilities in these laser-fast-beam interactions, two kinds of experiments are interesting. The first one simply reduces the observed linewidths by going to long-lived excited levels. Resonances have been observed in $^{238}\text{U II}$ in a V configuration²² with upper-level lifetimes of several μsec comparable to the transit-time broadening. The second type concerns resonant, stimulated Raman scattering, recently demonstrated by Thomas *et al.*²³ to have a unique resolution capability. In a resonant, inverted- V configuration in a fast-beam-laser setup, this experiment can be performed with one laser, the Doppler shifts providing a frequency difference in the Raman scattering of $\simeq 3$ THz. Performed on an optically cooled fast beam, the second-order Doppler broadening can be reduced below the transit-time broadening, which is of the order of 10–100 kHz.

- *Permanent address: Department of Physics, University of Toledo, Toledo, Ohio 43606.
- ¹H. J. Andrä, A. Gaupp, and W. Wittman, *Phys. Rev. Lett.* **31**, 501 (1973).
- ²S. L. Kaufman, *Opt. Commun.* **17**, 309 (1976).
- ³K. R. Anton, S. L. Kaufman, W. Kelmpf, G. Monizzi, R. Neugart, E.-W. Otten, and B. Schinzler, *Phys. Rev. Lett.* **40**, 642 (1978).
- ⁴W. H. Wing, G. A. Ruft, W. E. Lamb, and J. Spezeski, *Phys. Rev. Lett.* **36**, 1488 (1976).
- ⁵E.-W. Otten, in *Some Recent Developments in Laser Spectroscopy of Unstable Isotopes*, proceedings of the Fifth International Conference on Nuclei far from Stability, edited by P. G. Hansen and O. B. Nielsen (CERN, Geneva, 1981), p. 3.
- ⁶E. G. Meyers, P. Kuske, H. J. Andrä, I. A. Armour, N. A. Jelley, H. A. Klein, J. D. Silver, and E. Träbert, *Phys. Rev. Lett.* **47**, 87 (1981).
- ⁷O. Poulsen, T. Andersen, S. M. Bentzen, and U. Nielsen, *Phys. Rev. A* **24**, 2523 (1981).
- ⁸O. Poulsen and P. S. Ramanujam, *Phys. Rev. A* **14**, 1463 (1976).
- ⁹J. C. Bergquist, S. A. Lee, and J. L. Hall, *Phys. Rev. Lett.* **38**, 170 (1977); G. Borghs, P. de Bisschop, J.-M. Van den Cruyce, M. Van Hove, and R. E. Silverans, *Phys. Rev. Lett.* **46**, 1074 (1981).
- ¹⁰J. J. Snyder and J. L. Hall, *Proceedings of the Second International Conference on Laser Spectroscopy, Megève, France, 1975*, edited by S. Haroche *et al.* (Springer-Verlag, Heidelberg, 1976), p. 6.
- ¹¹M. Dufay, M. Carré, M. L. Gaillard, G. Meunier, H. Winter, and A. Zgainsky, *Phys. Rev. Lett.* **37**, 1678 (1976); F. Beguin-Renier, J. Désesquelles, and M. L. Gaillard, *Phys. Scr.* **18**, 21 (1978).
- ¹²T. D. Gaily, J. M. Coggiole, J. R. Peterson, and K. T. Gillen, *Rev. Sci. Instrum.* **51**, 1168 (1980).
- ¹³O. Poulsen and N. I. Winstrup, *Phys. Rev. Lett.* **47**, 1522 (1981).
- ¹⁴T. W. Hänsch, *Spectroscopia non Lineare, Proceedings of the International School of Physics "Enrico Fermi"* Course number 64 (North-Holland, New York, 1977), Vol. 64, p. 17.
- ¹⁵V. S. Letokhov and C. P. Chebotayev, *Non-Linear Laser Spectroscopy*, Springer Series in Optical Sciences, edited by D. L. MacAdam (Springer-Verlag, Heidelberg, 1977), Vol. 4, p. 185.
- ¹⁶P. G. Pappas, M. M. Burns, D. D. Hinshelwood, M. S. Feld, and D. E. Murnich, *Phys. Rev. A* **21**, 1955 (1980).
- ¹⁷R. M. Schectman, D. R. Schoffstall, D. G. Ellis, and D. A. Chojnacki, *J. Opt. Soc. Am.* **63**, 80 (1973).
- ¹⁸R. G. Brewer and E. L. Hahn, *Phys. Rev. A* **11**, 1641 (1975).
- ¹⁹V. Kaufman and B. Edlén, *J. Phys. Chem. Ref. Data* **3**, 825 (1974).
- ²⁰J. L. Hall and S. A. Lee, *Appl. Phys. Lett.* **29**, 367 (1976).
- ²¹P. Juncar and J. Pinard, *J. Appl. Phys.* (in press).
- ²²O. Poulsen, in *Atomic Physics 8*, edited by I. Lindgren, S. Svanberg, and A. Rosén (Plenum, New York, London, 1983).
- ²³J. E. Thomas, P. R. Hemmer, S. Ezekiel, C. C. Leiby, Jr., R. H. Picard, and C. R. Willis, *Phys. Rev. Lett.* **48**, 867 (1982).